Pattern coarsening in a $2D$ hexagonal system

C. Harrison[1], D. E. Angelescu[1], M. Trawick[1], Zhengdong Cheng[1],
D. A. Huse[1], P. M. Chaikin[1], D. A. Vega[2], J. M. Sebastian[2],
R. A. Register[2] and D. H. Adamson[3]

[1] *Department of Physics, Princeton University - Princeton, USA*
[2] *Department of Chemical Engineering, Princeton University - Princeton, USA*
[3] *Princeton Materials Institute, Princeton University - Princeton, USA*

Abstract. – We have studied the ordering dynamics of a two-dimensional system which consists of a single layer of spherical block copolymer microdomains in a thin film. We follow the annealing process after a quench from the disordered state by electron microscopy and time-lapse atomic force microscopy. At late times the orientational correlation length ξ_6 of the microdomain lattice exhibits a $t^{1/4}$ temporal power law. We compare the time evolution of the densities of dislocations, disclinations and the dislocation orientational correlation function. While most disclinations condense into dislocations and most dislocations condense into "grain boundaries", the dynamics appear to involve the interplay of disclinations and lines of dislocations. Rather than isolated grains shrinking, the most frequently observed process is the collapse of a smaller grain which resides on the boundary of two larger grains.

Over the past several decades there have been significant advances in our understanding of defect-mediated melting in two dimensions, both with striped and crystalline phases [1–5]. However, there remain many open questions concerning both the kinetics and mechanisms for ordering into the equilibrium states. We have recently shown that insights into the coarsening dynamics of striped (2D smectic) phases can be gained by studies of monolayer films of diblock copolymers and particularly from time-lapse atomic force microscopy (AFM) [6]. Diblock copolymers consist of two homogeneous but chemically distinct blocks connected with a covalent bond; for components which are sufficiently dissimilar, microphase separation occurs in the melt, into morphologies such as spheres or cylinders of the minor component in a matrix of the majority block [7]. The diblock systems are periodic on a 40 nanometer length scale and cover square centimeters so that large regions free of edge effects are available for investigation and application by lithographic processes [8–13]. In the striped system (in-plane block copolymer cylinders) we were able to show that the orientational correlation length was directly related to the average distance between disclinations and that both grew as $t^{1/4}$. We related this exponent to the annihilation of disclination quadrupoles [6]. The present study was undertaken to obtain a similar elucidation of the coarsening of patterns with hexagonal
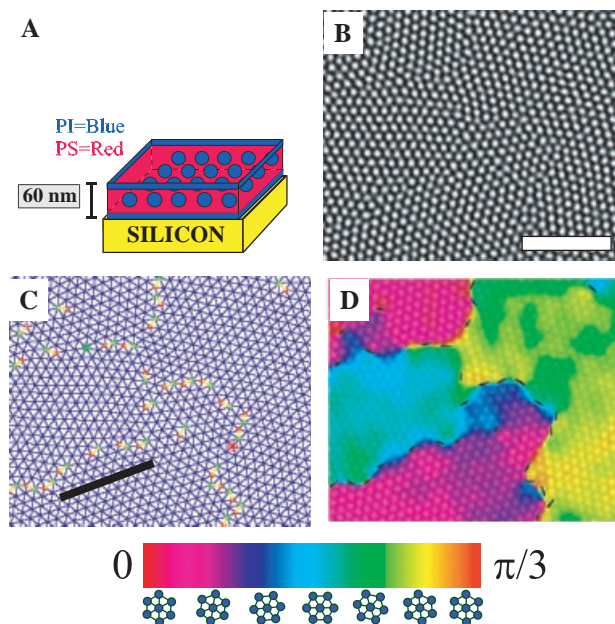
Fig. 1 – Pattern formation and analysis of copolymer thin film. (A) Schematic of single layer of polyisoprene (PI, denoted blue) spherical microdomains in a polystyrene (PS, denoted red) matrix. Note PI wetting layers at top and bottom interfaces. (B) Unprocessed SEM data of PS-PI 68-12 copolymer film. The OsO_4-stained spheres produce a higher electron yield and appear lighter than the unstained PS matrix. Bar = 300 nm. (C) Delaunay triangulation where the edges and vertices with six nearest neighbors are blue, vertices with five nearest neighbors red, and vertices with seven nearest neighbors green. Edge orientation is used to measure $\theta(r)$. Elementary dislocations are comprised of a 5 and 7 connected with a yellow edge. Note that edge dislocations along a grain boundary show a persistent orientation (indicated by the black bar). (D) Color map of the local lattice orientation where the colors of the spectrum indicate a range from 0 to $\pi/3$. Dislocations are indicated in black for clarity and the electron microscope image is shown in the background.

symmetry (block copolymer spheres). Here we show a similar $t^{1/4}$ power law for the orientational correlation length but different power laws for the distance between either dislocations or disclinations. We also investigate the idea of crystalline "grains" separated by dislocations arranged in grain boundaries and find it inadequate to explain the relationship between dislocation densities, correlation lengths and orientational order.

Our model system consists of asymmetric polystyrene-polyisoprene (PS-PI) copolymers that were synthesized via living anionic polymerization with a mass of 68 kg/mol for the PS block and 12 kg/mol for the PI block to form PI spheres in a PS matrix (PS-PI 68-12). Copolymers were applied (film thickness ca. 65 nm) to carbon-coated silicon substrates via spin coating from a disordered state in toluene, a good solvent for both blocks. Order was induced through vacuum annealing above the glass transition temperature (measured by differential scanning calorimetry (DSC) to be 373 K), producing the structure which is schematically shown in fig. 1A, containing a single layer of spherical microdomains as confirmed previously [14]. By comparison with other PS-PI diblocks of similar composition [15], the order-disorder transition temperature of PS-PI 68-12 exceeds 500 K, and is experimentally inaccessible due to polymer degradation. After annealing, microdomains were preferentially stained with the vapors of OsO_4 to provide contrast for electron microscopy. The microdomain
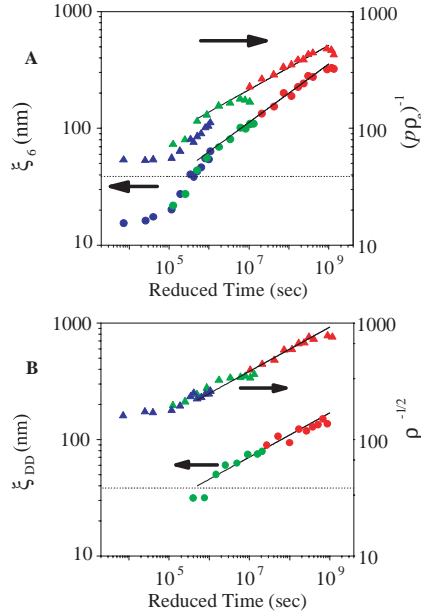
Fig. 2 – Data from PS-PI 68-12. (A) Time dependence of the orientational correlation length ξ_6 (circles) and $(p\rho_\epsilon)^{-1}$ (triangles). The data from three temperatures (398, 413, and 443 K) are plotted in blue, green, and red, respectively. Times for the two higher temperatures have been shifted to 398 K according to the WLF equation. For reduced times greater than 10^5 seconds, $\xi_6 \sim t^{1/4}$ and $(p\rho_\epsilon)^{-1} \sim t^{1/5}$. We have approximated p to be 100 nm. (B) The correlation length measured from the dislocation vector field (circles, left axis) and the average distance between disclinations (triangles, right axis). Both scale as $t^{1/5}$. For both panels, the solid black lines correspond to the power laws obtained from fitting the data. The horizontal dashed lines correpond to one repeat spacing.

pattern was examined with an imaging technique which uniformly etches away the free surface wetting layer of PI with low-power, low-pressure, CF_4-based reactive ion etching [16] (Applied Materials, Inc.) to expose the microdomains to the surface for imaging with a LEO/Zeiss 982 Scanning Electron Microscope (SEM) [14, 17]. Figure 1B shows a representative image where the stained PI spheres appear lighter due to a higher electron yield and can be seen in a poly-domain configuration. The lattice constant a for the hexagonal pattern is 39 nm as measured from the wave number of dominant intensity in Fourier space.

The orientational correlation length (ξ_6) of the coarsening pattern was measured as a function of time to quantify the degree of microdomain order. This was accomplished by annealing multiple samples in parallel for varying lengths of time and collecting many SEM images from each sample. Standard image processing techniques were employed to identify each sphere center with sub-pixel accuracy [18]. The local orientational order parameter, $\psi(\vec{r}) = \exp[6i\theta(\vec{r})]$, was computationally measured, where θ is the inter-sphere bond orientation (obtained by De-launay triangulation [19], see fig. 1C-D) and $\vec{r}$ is the position [1]. The azimuthally averaged correlation function $g_6(r) = \langle \psi(0)\psi(r) \rangle$ was then calculated and the correlation length ξ_6 was measured by fitting with $\exp[-r/\xi_6]$ [20]. Three annealing temperatures (398 K, 413 K, 443 K) were examined and the time dependence of the correlation length is plotted in fig. 2A in blue, green, and red circles, respectively. The annealing times for the data at the two higher temperatures have been shifted according to the Williams-Landel-Ferry (WLF) equation to account for changes in segmental mobility within the PS matrix. According to the WLF

equation [21], the shift factor, a_T, can be expressed as

$$\log a_T = -c_1^0(T - T_0)/(c_2^0 + T - T_0). \tag{1}$$

For PS ($T_g = 373\,\text{K}$), the constants [21] are $c_1^0 = 13.7$, $c_2^0 = 50.0\,\text{K}$, and $T_0 = 373\,\text{K}$, producing shift factors of 33 and 2700 for $413\,\text{K}$ and $443\,\text{K}$, respectively, relative to the reference temperature, $373\,\text{K}$. After multiplying the annealing times by the calculated shift factors, the data collapse onto a curve that results in a one-quarter temporal power law (0.25 ± 0.01) for ξ_6 greater than one lattice constant. While temperature-dependent changes in interblock segregation strength also influence chain diffusivity, for PS-PI 68-12 over the temperature range of interest, the PS segmental mobility is calculated to be the dominant factor by far, as reflected in the satisfactory collapse of the data in fig. 2 [22,23]. The data associated with the lowest temperature show a reduced scaling exponent, most likely due to the small values of ξ_6 (comparable to the lattice constant a) under these annealing conditions. Similar exponents have been measured from simulations [24]. While the coarsening, non-equilibrium structures described in the present work do not clearly reflect the underlying equilibrium state, independent measurements on samples carefully annealed in a temperature gradient [25] reveal that the ordered phase formed below the ODT temperature in single-layer films of PS-PEP 3-24 is hexatic, rather than crystalline, in agreement with a previous report for another diblock copolymer system [5].

The similarity of both the measured kinetic exponents and the topological defects (*e.g.* dislocations and disclinations) in both hexatic and smectic systems suggests that coarsening is driven by topological rather than morphological properties [6]. A casual inspection of the Delaunay triangulation of well-coarsened patterns (fig. 1C) reveals the existence of grain boundaries (albeit poorly-defined in regions), which are primarily composed of topological defects referred to as dislocations. Dislocations (density ρ_ϵ) were identified by pairs of five-fold and seven-fold vertices that shared a triangulation edge (yellow). Disclinations (density ρ) were identified as free, rather than bound into a dislocation, if all nearest neighbors were void of defects, or engaged in other dislocations. Free disclinations were seen at a lower density (1/5 that of dislocations) and with strain fields that did not dramatically dominate the image, unlike that which we observed in a striped system [6]. The mean distance between disclinations ($\rho^{-1/2}$) was measured to follow a $t^{1/5}$ power law, suggesting that the origin of ξ_6's behavior is more subtle (fig. 2B).

To try to understand the role of defects in pattern coarsening, an alternative microscopy technique was employed that was non-destuctive and enabled us to observe the evolution of individual grains. We took advantage of the modulus difference between two blocks in a related copolymer system and used tapping mode AFM to image the microdomain pattern (PS-PI 68-12 cannot be imaged in such a convenient, non-destructive manner). A hydrogenated diblock was employed which consisted of PS spheres in a poly (ethylene-*alt*-propylene), PEP, matrix (denoted PS-PEP 3-24) [15]. We measured the order-disorder temperature (ODT) of PS-PEP 3-24 via small-angle X-ray scattering to be $394 \pm 2\,\text{K}$ [15], so PS-PEP 3-24 is less strongly segregated than PS-PI 68-12, and the rubbery matrix imparts more rapid coarsening dynamics. Despite the differences in segregation strength, no qualitative differences in the types of defects present or in the coarsening dynamics were observed. The glass transition temperature was estimated to be $320\,\text{K}$ by comparison with other PS-containing strongly segregated diblocks of comparable molecular weights (DSC is not sufficiently sensitive to reveal the transition) [26]. Spin-coated samples were imaged at ambient temperature, annealed in air at $343\,\text{K}$ on a temperature-controlled heater stage mounted on the AFM [27,28], and then re-imaged after cooling to examine the coarsening microdomain pattern. By re-
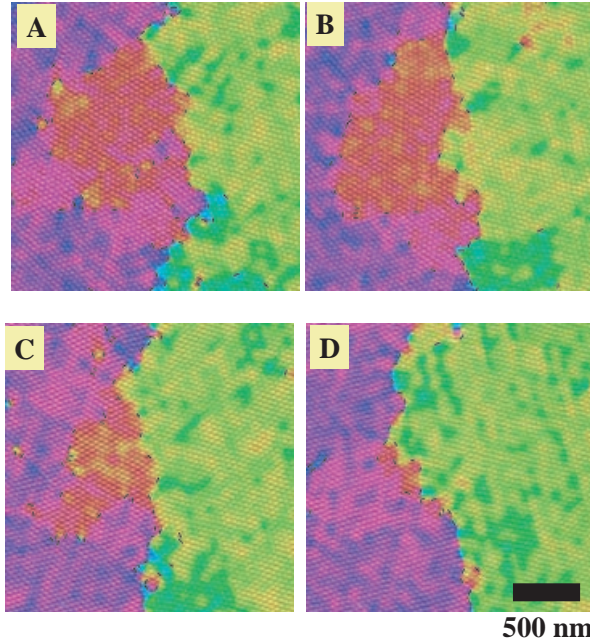
Fig. 3 – Time sequence AFM images of PS-PEP 3-24 showing grain annihilation in the same representation scheme as in fig. 1D. Panel A shows a grain in the center of the image (red) which disappears with annealing in panels B-D. The larger grains on either side have absorbed the smaller grain. The dislocations (designated by black lines) associated with this grain in panel A also disappear by panel D.

peating this cycle dozens of times and reimaging the same area we observed the evolution of individual grains.

The typical coarsening process we observe is shown in fig. 3. Here we see two large grains on the left and right sides of the figure, with two small grains lying on the boundary between them. The motion of the grain boundaries is rather stochastic, but the grains shrink and are absorbed into the larger grain boundary which remains. In the process, dislocations are annihilated as are the disclinations at the "forks" where the grain boundaries split. In many cases it appears that the splitting of the boundary is "zipped up," possibly by an attraction between the disclinations at the forks. The net effect is that smaller grains collapse into the grain boundary between larger grains and the process is then repeated at larger scales and longer times. Hence insight into the coarsening mechanism may be obtained by quantitative analysis of defect densities.

We have demonstrated that coarsening involves an increase in $\xi_6(t)$ as well as grain annihilation. These two processes are linked as lines of dislocations that are organized into grain boundaries produce a discontinuous lattice rotation upon crossing a grain boundary, thereby affecting ξ_6. The rotation of one grain relative to its neighbor is $\tan \delta\theta \sim a/p$, where p is the distance between dislocations on the grain boundary and a is the lattice spacing. We now examine the relationship between ξ_6 and ρ_ϵ by assuming that grains are *well defined*, separated by dislocations that are clustered onto grain boundaries, and that p is constant. In our case, the distance between dislocations on the grain boundary is small; $p/a \sim 2$–3, $\delta\theta \sim 30°$ so that the lattice orientation is randomized in traversing a single grain boundary. If grains are of size L, then the area per grain is $\sim L^2$, the number of dislocations per grain is $\sim L/p$, and the density of dislocations is $\rho_\epsilon \sim 1/pL$. In this case we expect that $\xi_6 \sim L \sim 1/(p\rho_\epsilon)$. In fig. 2A

we have plotted ξ_6 and $1/(p\rho_\epsilon)$ as a function of time for our samples with p approximated as 100 nm. The similarity of the magnitudes of $\xi_6(t)$ and $1/(p\rho_\epsilon(t))$ (circles and triangles, respectively, in fig. 2A) is evidenced by shapes of the curves but the kinetics differ significantly as $\xi_6 \sim t^{1/4}$ and $1/(p\rho_\epsilon) \sim t^{1/5}$ (0.19 ± 0.01). Using a t-distribution (student test) at the 99.5% confidence level we can soundly reject the "null hypothesis" that the exponents from $1/(p\rho_\epsilon)$ and $\xi_6(t)$ display the same exponent. We emphasize that our claim is not that the growth mechanisms necessarily follow power laws (such an assertion would require a much greater measurement range than is experimentally possible here) but rather that the growth rates of ξ_6 and $1/(p\rho_\epsilon)$ differ significantly. One possibility is that the average value of p/a is decreasing during pattern coarsening, which would result from a tendency towards higher-angle grain boundaries. However, measurements reveal that the distance between dislocations along grain boundaries (p/a) *increases* slightly (less than 35%) during the experiment, suggesting that other factors may be responsible for the difference. The key difference between grain boundaries in a more traditional metallic, three-dimensional system and the 2D copolymer system here is the diffuse quality of the latter. While it is straightforward to select a defect-free region, grains are often not well separated by continuous lines of closely spaced dislocations. Additionally, measurements on large grains (for both copolymer systems discussed here) revealed that each grain has good orientational order (non-zero correlation function intensity at length scales comparable to the grain size) but translational order decays within a few lattice constants, as expected for a hexatic structure, again making it difficult to precisely locate a grain boundary by a phase shift in a mass density wave.

Since ξ_6 does not scale with the same exponent as the area per dislocation, we examined the length scale set by the clustering of dislocations on grain boundaries. Like-signed dislocations share a common orientation over a characteristic distance which is indicated by the black bar in fig. 1C. The orientation of a dislocation can be determined by treating the five as the head of a vector and the seven as the tail; the entire set of dislocations can then be used create a vector field. To measure this characteristic orientational dislocation distance we evaluated the orientational correlation function of the vector fields of dislocations, denoted $g_{DD}(r)$, which is similar to $g_6(r)$ except that $\theta(r)$ corresponds here to the orientational field of the dislocations and that the six-fold degeneracy is removed from $\psi(r)$ as the dislocation orientation is a vector. All quantitative analysis in this paper, including that performed on $g_{DD}(r)$, was obtained from PS-PI 68-12 data. We fit $g_{DD}(r)$ with an exponential decay in a similar manner as $g(r)$ to measure ξ_{DD}. While the low density of dislocations gives rise to a much higher noise level in the correlation function, we found that the magnitudes of ξ_6 and ξ_{DD} are within factors of two to three of each other but ξ_{DD} grows more slowly than ξ_6, in fact $\xi_{DD} \sim (p\rho_\epsilon)^{-1}$ (figs. 2A-B). The fact that ξ_6, ξ_{DD}, and $1/(p\rho_\epsilon)$ do not scale together, even though they are close, brings into question whether the concept of grains is well defined in our system.

In summary, we have shown that the pattern coarsening of a single layer of spherical microdomains proceeds via a set of fractional power laws. The orientational correlation length ξ_6 grows as $\sim t^{1/4}$, while the distance between disclinations increases as $\sim t^{1/5}$. Time-lapse AFM shows that pattern coarsening is largely stochastic and that the dominant coarsening process is the collapse of small grains into the grain boundaries of larger grains.

$$* * *$$

REFERENCES

[1] NELSON D. R. and HALPERIN B. I., *Phys. Rev. B*, **19** (1979) 2457.
[2] HALPERIN B. I. and NELSON D. R., *Phys. Rev. Lett.*, **41** (1978) 121.
[3] MURRAY C., in *Bond-Orientational Order in Condensed Matter Systems*, edited by STRAND-BERG K. (Springer-Verlag, New York) 1992.
[4] SEGALMAN R. A., HEXEMER A., HAYWARD R. C. and KRAMER E. J., *Macromolecules*, **36** (2003) 3272.
[5] SEGALMAN R. A., HEXEMER A. and KRAMER E. J., *Phys. Rev. Lett.*, **91** (2003) 196101.
[6] HARRISON C., ADAMSON D. H., CHENG Z., SEBASTIAN J. M., SETHURAMAN S., HUSE D. A., REGISTER R. A. and CHAIKIN P. M., *Science*, **290** (2000) 1558.
[7] HAMLEY I. W., *The Physics of Block Copolymers*, 1st edition (Oxford University Press, New York) 1998.
[8] HARRISON C., PARK M., CHAIKIN P. M., REGISTER R. A. and ADAMSON D. H., *J. Vac. Sci. Technol. B*, **16** (1998) 544.
[9] PARK M., CHAIKIN P. M., REGISTER R. A. and ADAMSON D. H., *Appl. Phys. Lett.*, **79** (2001) 257.
[10] LI R. R., DAPKUS P. D., THOMPSON M. E., JEONG W. G., HARRISON C. K., CHAIKIN P. M., REGISTER R. A. and ADAMSON D. H., *Appl. Phys. Lett.*, **76** (2000) 1689.
[11] GUARINI K. W., BLACK C. T., ZHANG Y., KIM H., SIKORSKI E. M. and BABICH I. V., *J. Vac. Sci. Technol. B*, **20** (2002) 2788.
[12] ASAKAWA K., HIRAOKA T., HIEDA H., SAKURAI M., KAMATA Y. and NAITO K., *J. Photopolym. Sci. Technol.*, **15** (2002) 465.
[13] CHENG J. Y., ROSS C. A., THOMAS E. L., SMITH H. I. and VANCSO G. J., *Appl. Phys. Lett.*, **81** (2002) 3657.
[14] HARRISON C., PARK M., CHAIKIN P., REGISTER R., ADAMSON D. and YAO N., *Polymer*, **30** (1998) 2733.
[15] SEBASTIAN J. M., LAI C., GRAESSLEY W. W. and REGISTER R. A., *Macromolecules*, **35** (2002) 2707.
[16] SZE S., *VLSI Technology*, 2nd edition (McGraw-Hill, New York) 1988, p. 184.
[17] HARRISON C., PARK M., CHAIKIN P. M., REGISTER R. A. and ADAMSON D. H., *Macromolecules*, **31** (1998) 2185.
[18] CROCKER J. C. and GRIER D. G., *J. Colloid Interface Sci.*, **179** (1996) 298.
[19] O'ROURKE J., *Computational Geometry in C*, 2nd edition (Cambridge University Press, New York) 1998.
[20] HALPERIN B. I., in *Proceedings of the Kyoto Summer Institute 1979 - Physics of Low Dimensional Systems*, edited by NAGAOKA Y. and HIKAMI S. (Publications Office, Progress of Theoretical Physics, Kyoto) 1979, p. 53.
[21] FERRY J. D., *Viscoelastic Properties of Polymers*, 3rd edition (John Wiley and Sons, New York) 1980.
[22] YOKOHAMA H. and KRAMER E. H., *Macromolecules*, **31** (1998) 7871.
[23] SEBASTIAN J. M., GRAESSLEY W. W. and REGISTER R. A., *J. Rheol.*, **46** (2002) 863.
[24] YOKOJIMA Y. and SHIWA Y., *Phys. Rev. E*, **65** (2002) 056308.
[25] ANGELESCU D. E., PhD Thesis, Princeton University (2003).
[26] LU Z. H. and KRAUSE S., *Macromolecules*, **15** (1982) 112.
[27] A prototype thermal accessory from Digital Instruments. This has subsequently been replaced with the Thermal Accessory for Multimode and High Temperature Accessory for Multimode.
[28] HARRISON C., CHENG Z. D., SETHURAMAN S., HUSE D. A., CHAIKIN P. M., VEGA D. A., SEBASTIAN J. M., REGISTER R. A. and ADAMSON D. H., *Phys. Rev. E.*, **66** (2002) 011706.